Méthodes numérique de la mécanique/*Computational Mechanics*

Numerical Simulation of the Motion of a Ball Falling in an Incompressible Viscous Fluid

Tsorng-Whay PAN

University of Houston, Department of Mathematics, Houston, Texas 77204-3476, USA

Abstract. In this note we discuss the application of a Lagrange multiplier based fictitious domain method to the numerical simulation of the motion of a ball falling in an incompressible viscous fluid; the motion is due to the hydrodynamical forces and gravity. The numerical results of the terminal velocity of a ball falling in a circular cylinder are in quantitative agreement with the experimental results for Reynolds numbers less than 35.

Simulation numérique de la chute d'une sphère pesante dans un fluide visqueux incompressible

Résumé. Dans cette note, on décrit l'application d'une méthode de domaine fictif avec multiplicateurs de Lagrange distribués à la simulation numérique de la chute d'une sphère dans un fluide visqueux incompressible; le mouvement de la sphère est du aux forces hydrodynamiques et à la pesanteur. Les valeurs calculées de la vitesse finale, pour la chute d'une sphère contenue dans un cylindre circulaire, sont en accord, quantitativement, avec les valeurs experimentales données dans [7], pour des nombres de Reynolds inférieurs à 35.

1 Introduction

In this note, we consider the numerical simulation of the motion of a ball falling in an incompressible viscous fluid by a *distributed Lagrange multiplier/fictitious domain method* (see refs. [1], [2], and [3]). The motion of the ball is not known a priori and is due to the *hydrodynamical forces* and gravity. In the simulation we do not need to compute the hydrodynamical forces explicitly, since the interaction between fluid and rigid bodies is implicitly modeled by the global variational formulation at the foundation of the methodology employed here. Also we avoid generating three dimensional boundary fitted grids for different positions of the ball, but just need a simple structured grid and the geometrical relation between the ball and the grid. In [1], [2], and [3], this methodology has

Note présentée par Roland Glowinski.

been able to: simulate the drafting, kissing, and tumbling, a fundamental phenomenon of two spherical particles falling in Newtonian fluids [4], in two and three dimensions, and particulate flow with the number of particles on the order of 10^3 in 2-D and 10^2 in 3-D. In order to compare numerical results with experimental ones and obtain more quantitative validation of our methodology, we are going to consider a well documented case, namely balls of different sizes falling in an incompressible viscous fluid contained in a cylinder.

2 A fictitious domain formulation of the model problem.

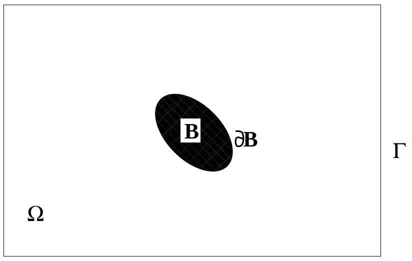

Figure 1: An example of two-dimensional flow region with one rigid body.

Let $\Omega \subset \mathbb{R}^d (d = 2, 3$; See Figure 1 for a particular case where $d = 2)$ be a space region; we suppose that Ω is filled with a *Newtonian viscous incompressible* fluid (of *density* ρ_f and *viscosity* ν_f) and contains a moving rigid body B of *density* ρ_s; the incompressible viscous flow is modeled by the *Navier-Stokes equations* and the motion of the ball is described by the *Euler's equations* (an almost direct consequence of Newton's laws of motion). Let us first define the following functional spaces

$$W_{\mathbf{g}_0}(t) = \{\mathbf{v} | \mathbf{v} \in (H^1(\Omega))^d, \ \mathbf{v} = \mathbf{g}_0(t) \ on \ \Gamma\},$$
$$L_0^2(\Omega) = \{q | q \in L^2(\Omega), \ \int_\Omega q d\mathbf{x} = 0\}, \quad \Lambda(t) = (H^1(B(t)))^d;$$

then the *fictitious domain formulation with distributed Lagrange multipliers* for flows around freely moving rigid bodies (see [3] for detail) is as follows

For a.e. $t > 0$, *find* $\{\mathbf{u}(t), p(t), \mathbf{V_G}(t), \mathbf{G}(t), \boldsymbol{\omega}(t), \boldsymbol{\lambda}(t)\}$ *such that*

$$\mathbf{u}(t) \in W_{\mathbf{g}_0}(t), \ p(t) \in L_0^2(\Omega), \ \mathbf{V_G}(t) \in \mathbb{R}^d, \ \mathbf{G}(t) \in \mathbb{R}^d, \ \boldsymbol{\omega}(t) \in \mathbb{R}^3, \ \boldsymbol{\lambda}(t) \in \Lambda(t) \tag{2.1}$$

and

$$\begin{cases} \rho_f \displaystyle\int_\Omega \frac{\partial \mathbf{u}}{\partial t} \cdot \mathbf{v} d\mathbf{x} + \rho_f \int_\Omega (\mathbf{u} \cdot \boldsymbol{\nabla}) \mathbf{u} \cdot \mathbf{v} d\mathbf{x} - \int_\Omega p \boldsymbol{\nabla} \cdot \mathbf{v} d\mathbf{x} \\ \quad + 2\nu_f \displaystyle\int_\Omega \mathbf{D}(\mathbf{u}) : \mathbf{D}(\mathbf{v}) d\mathbf{x} \ - (\boldsymbol{\lambda}, \mathbf{v} - \mathbf{Y} - \boldsymbol{\theta} \times \mathbf{G}\mathbf{x})_{\Lambda(t)} \\ \quad + (1 - \dfrac{\rho_f}{\rho_s})[M \dfrac{d\mathbf{V_G}}{dt} \cdot \mathbf{Y} + (\mathbf{I} \dfrac{d\boldsymbol{\omega}}{dt} + \boldsymbol{\omega} \times \mathbf{I}\boldsymbol{\omega}) \cdot \boldsymbol{\theta}] - \mathbf{F}^r \cdot \mathbf{Y} \\ = (1 - \dfrac{\rho_f}{\rho_s}) M \mathbf{g} \cdot \mathbf{Y} + \rho_f \displaystyle\int_\Omega \mathbf{g} \cdot \mathbf{v} d\mathbf{x}, \ \forall \mathbf{v} \in (H_0^1(\Omega))^d, \ \forall \mathbf{Y} \in \mathbb{R}^d, \ \forall \boldsymbol{\theta} \in \mathbb{R}^3, \end{cases} \tag{2.2}$$

$$\int_\Omega q\nabla\cdot\mathbf{u}(t)d\mathbf{x}=0,\ \forall q\in L^2(\Omega), \tag{2.3}$$

$$\frac{d\mathbf{G}}{dt}=\mathbf{V_G}, \tag{2.4}$$

$$(\boldsymbol{\mu},\mathbf{u}(t)-\mathbf{V_G}(t)-\boldsymbol{\omega}(t)\times\mathbf{G}(t)\mathbf{x})_{\Lambda(t)}=0,\ \forall\boldsymbol{\mu}\in\Lambda(t), \tag{2.5}$$

$$\mathbf{V_G}(0)=\mathbf{V}^0,\ \boldsymbol{\omega}(0)=\boldsymbol{\omega}^0,\ \mathbf{G}(0)=\mathbf{G}^0; \tag{2.6}$$

$$\mathbf{u}(\mathbf{x},0)=\mathbf{u}_0(\mathbf{x}),\ \forall\mathbf{x}\in\Omega\backslash\overline{B(0)}\ \textit{and}\ \mathbf{u}(\mathbf{x},0)=\mathbf{V}^0+\boldsymbol{\omega}^0\times\mathbf{G}^0\mathbf{x},\ \forall\mathbf{x}\in\overline{B(0)}. \tag{2.7}$$

In (2.1)-(2.7), $\mathbf{u}(=\{u_i\}_{i=1}^d)$ and p denote velocity and pressure respectively, $\boldsymbol{\lambda}$ a Lagrange multiplier, $\mathbf{D}(\mathbf{v})=(\nabla\mathbf{v}+\nabla\mathbf{v}^t)/2$, $\mathbf{g}$ is the gravity, $\mathbf{V_G}$ is the *translation velocity* of the rigid body B, $\boldsymbol{\omega}$ is the *angular velocity* of B, M is the mass of the rigid body, $\mathbf{I}$ is the *inertia tensor* of the rigid body at $\mathbf{G}$, $\mathbf{G}$ being the center of mass of B; $\boldsymbol{\omega}(t)=\{\omega_i(t)\}_{i=1}^3$ and $\boldsymbol{\theta}=\{\theta_i\}_{i=1}^3$ if $d=3$, while $\boldsymbol{\omega}(t)=\{0,0,\omega(t)\}$ and $\boldsymbol{\theta}=\{0,0,\theta\}$ if $d=2$. In order to treat possible *collisions* between B and Γ , $\mathbf{F}^r$ is a *lubrication force* (see [2]) imposed on B by Γ (in those parts of Γ that B cannot cross). From the rigid body motion of B, $\mathbf{g}_0$ has to satisfy $\displaystyle\int_\Gamma \mathbf{g}_0\cdot\mathbf{n}d\Gamma=0$, where $\mathbf{n}$ denotes the unit vector of the outward normal at Γ (we suppose the *no-slip* condition on ∂B). We also use, if necessary, the notation $\phi(t)$ for the function $\mathbf{x}\to\varphi(\mathbf{x},t)$.

Remark 2.1. The hydrodynamics forces and torque imposed on the rigid body by the fluid are built in (2.1)-(2.7) implicitly (see [3] for detail), we do not need to compute them explicitly in the simulation. Since in (2.1)-(2.7) the flow field is defined on the entire domain Ω, it can be computed with a simple structured grid. Then by (2.5), we can enforce the rigid body motion in the region occupied by the rigid bodies via Langrange multipliers.

3 Space approximation and time discretization

Concerning the *space approximation* of problem (2.1)-(2.7) by a finite element method, we divide Ω, a rectangular cylinder, into a collection of cubes of edge length h where h is a *space discretization step*; and then divide each cube into six tetrahedra to obtain a finite element tetrahedrization $\mathcal{T}_h$ of Ω for velocity field and use similar procedure to get $\mathcal{T}_{2h}$ for pressure. Then we use P_1isoP_2 and P_1 finite elements for velocity field and pressure respectively in the space approximation. For the scalar product $<\cdot,\cdot>_{\Lambda(t)}$ in (2.1)-(2.7), we have used a collocation approach (see ref. [3]). A similar technique has been used to enforce Dirichlet boundary conditions by F. Bertrand, P.A. Tanguy and F. Thibault in [5].

After discretizing (2.1)-(2.7) in space, we obtain an initial value problem which contains four numerical difficulties to each of which can be associated a specific operator: (a) the incompressibility condition and the related unknown pressure, (b) an advection-diffusion term, (c) the rigid body motion of $B_h(t)$ and the related multiplier $\boldsymbol{\lambda}_h(t)$, and (d) the collision term $\mathbf{F}^r$. This initial value problem is a particular case of the following class of initial value problems

$$\frac{d\varphi}{dt}+A_1(\varphi,t)+A_2(\varphi,t)+A_3(\varphi,t)+A_4(\varphi,t)=f,\quad \varphi(0)=\varphi_0, \tag{3.1}$$

where the operators A_i can be *multivalued.* Among the many operator-splitting methods, we advocate the following fractional step scheme à la Marchuk-Yanenko (see, e.g., [6]):

for $n \geq 0$, *compute* φ^{n+1} *from* φ^n *via*

$$\frac{\varphi^{n+j/4} - \varphi^{n+(j-1)/4}}{\triangle t} + A_j(\varphi^{n+j/4}, (n+1)\triangle t) = f_j^{n+1}, \quad for\ j = 1, 2, 3, 4. \tag{3.2}$$

with $\sum_{j=1}^{4} f_j^{n+1} = f^{n+1}$, $\triangle t$ a time discretization step and the initial condition $\varphi^0 = \varphi_0$. This scheme is only first order accurate, but its low order accuracy is compensated by good stability and robustness properties. In the resulting discretized problem of (2.1)-(2.7), there are three major subproblems: (i) a divergence-free projection, (ii) a linear advection-diffusion problem, (iii) a rigid body motion projection. Each of these subproblems can be solved by conjugate gradient methods (see refs. [2] and [3] for detail).

4 Numerical experiments

We consider the simulation of a sedimenting ball in a circular cylinder of infinite length. This test case is well documented (see ref. [7]). The initial computational domain is $\Omega = (0,1) \times (0,2.5) \times (0,1)$, then it moves with the center of the ball. The cylinder is contained in the computational domain and we force velocity field outside the cylinder to be zero by another distributed Lagrange multiplier. The diameter of the cylinder is 1. The initial position of the ball is at $(0.5, 0.5, 0.5)$ which is on the central axis of the cylinder. The initial velocity and angular velocity of the ball are zero. The initial condition for the fluid flow is $\mathbf{u} = \mathbf{0}$. The density of the fluid is $\rho_f = 1.0$. We have chosen $\nu_f = 0.2$, 0.15, 0.1, 0.05, 0.02, and 0.01 as the viscosity of the fluid in the simulation. The diameters of the ball are 0.2, 0.3, or 0.4 and the density of the ball is either $\rho_s = 1.02$ or 1.14. The mesh size for the velocity field is $h_v = 1/64$. The mesh size for pressure is $h_p = 1/32$. The time step is $\triangle t = 0.0005$.

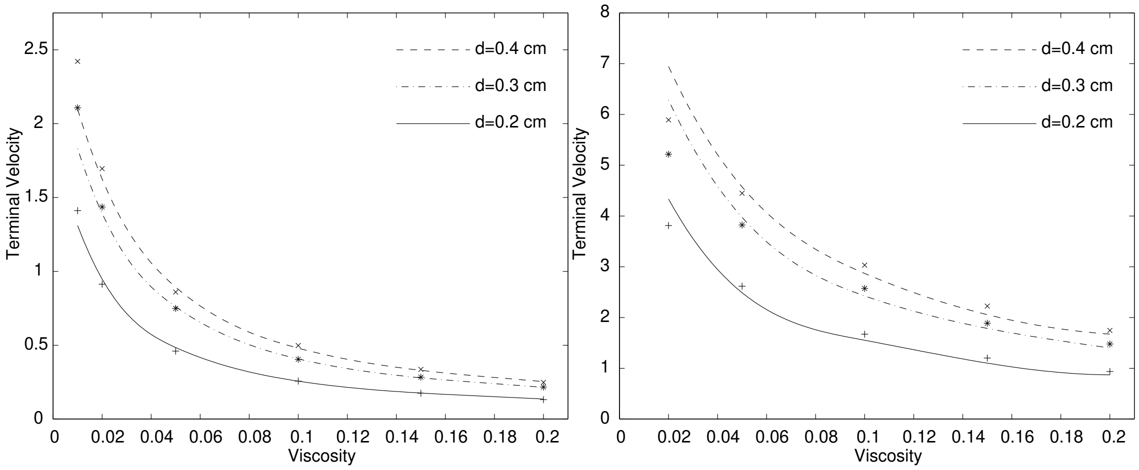

Figure 2: The measured terminal velocities (ref. [7]) of a ball falling along the central axis of the cylinder are described by the lines $(-)$, $(-\cdot-)$, and $(--)$ (the left one is associated with $\rho_s = 1.02$ and the right one is associated with $\rho_s = 1.14$). "+", "$*$", and "$\times$" denote the computed terminal velocities for the ball diameters d=0.2, 0.3 and 0.4 respectively.

In the simulation, the ball located initially on the central axis of the cylinder was released and fell freely in a gravitational field. There is no restriction to the motion of the ball, so it can move away from the central axis of the cylinder. In Figure 2, we have shown the results of computed terminal velocities and the terminal velocities of the ball of the density 1.02 with different diameters and viscosities. The *terminal velocities* are, from [7], obtained by multiplying the wall correction factor to the one of ball falling in unbounded region. The computed terminal velocities are in good agreement with the ones from [7] except the case where the viscosity is 0.01. The relative errors are less than 5% when the chosen viscosities are less than 0.01 (Reynolds numbera are less than 34). The results of the ball of the density 1.14 are shown in Figure 2. The computed terminal velocities are also in good agreement with the terminal velocities except the case where the viscosity is 0.02. The relative errors are less than 9% when the chosen viscosities are less than 0.02 (Reynolds numbers are less than 36). The large discrepancies occurred in the cases of the viscosity 0.01 ($\rho_s = 1.02$) and 0.02 ($\rho_s = 1.14$) might be caused by the fact that in the simulation the ball is away from the central axis of the cylinder.

We also considered the cases in which the density of ball is either $\rho_s = 1.3$, 1.4, or 1.5, the diameter of the ball is 0.2, and the viscosity is $\nu_f = 0.01$. After releasing the ball located initially on the central axis of the cylinder, it moves away from the central axis of the cylinder and then follows a spiral trajectory (e.g., see Figure 3). The Reynolds numbers are about 135, 161, and 180 for the density $\rho_s = 1.3$, 1.4, and 1.5 respectively.

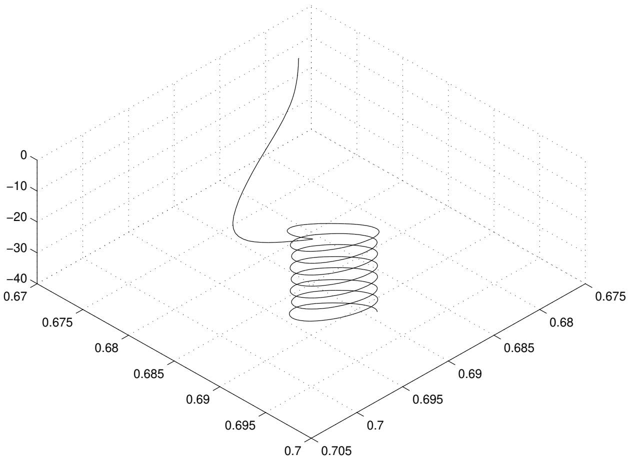

Figure 3: Spiral trajectory of a ball of the density 1.4 falling in a cylinder.

5 Acknowledgments

We acknowledge the helpful comments and suggestions of E. J. Dean, V. Girault, R. Glowinski, J. He, T. Hesla, H.H. Hu, D.D. Joseph, Y. Kuznetsov, B. Maury, and G. Rodin. We acknowledge also the support of the NSF/CTS-9873236, NSF HPCC Grand Challenge Grant ECS-9527123, Dassault Aviation, and the University of Houston (PEER grant 1-27682).

References

[1] R. Glowinski, T.I. Hesla, D.D. Joseph, T.W. Pan, J. Périaux, 'Distributed Lagrange multiplier methods for particulate flows', in M.O. Bristeau, G. Etgen, W. Fitzgibbon, J.L. Lions, J. Périaux and M.F. Wheeler (eds.), *Computational Science for the 21st Century*, John Wiley & Sons, Chichester, England, 1997, 270-279.

[2] R. Glowinski, T.-W. Pan, T. Hesla, D.D. Joseph, J. Périaux, 'A fictitious domain method with distributed Lagrange multipliers for the numerical simulation of particulate flows', in J. Mandel, C. Farhat, and X.-C. Cai (eds.), *Domain Decomposition Methods 10*, AMS, Providence, RI, 1998, 121-137.

[3] R. Glowinski, T.-W. Pan, T. Hesla, D.D. Joseph, 'A distributed Lagrange multiplier/fictitious domain method for particulate flows', *Int. J. Multiphase Flow* (to appear).

[4] A.F. Fortes, D.D. Joseph, T.S. Lundgren, 'Nonlinear mechanics of fluidization of beds of spherical particles', *J. Fluid Mech.*, **177**, 467-483 (1987).

[5] F. Bertrand, P.A. Tanguy, F. Thibault, 'A Three-dimensional fictitious domain method for incompressible fluid flow problem', *Int. J. Num. Meth. Fluids*, **25**, 719-736 (1997).

[6] G.I. Marchuk, 'Splitting and alternating direction methods', in P.G. Ciarlet and J.L. Lions (eds.), *Handbook of Numerical Analysis*, Vol. I, North-Holland, Amsterdam, 1990, 197-462.

[7] R. Clift, J.R. Grace, M.E. Weber, 'Bubbles, Drops, and Particles', Academic Press, New York, 1978, p. 113 and p. 226.